International Journal of Pharmaceutics 420 (2011) 34–42

Contents lists available at ScienceDirect

International Journal of Pharmaceutics

journal homepage: www.elsevier.com/locate/ijpharm

Enhanced dissolution of inhalable cyclosporine nano-matrix particles with mannitol as matrix former

Keishi Yamasaki[a,**], Philip Chi Lip Kwok[b], Kaori Fukushige[c], Robert K. Prud'homme[d], Hak-Kim Chan[b,*]

[a] Laboratory of Clinical Pharmaceutics, Faculty of Pharmaceutical Sciences, Sojo University, 4-22-1 Ikeda, Kumamoto, 860-0082, Japan
[b] Advanced Drug Delivery Group, Faculty of Pharmacy, Building A15, The University of Sydney, New South Wales 2006, Australia
[c] Graduate School of Pharmaceutical Sciences, Nagoya City University, 3-1 Tanabe-dori, Mizuho-ku, Nagoya, 467-8603, Japan
[d] Department of Chemical & Biological Engineering, A301 EQUAD, Princeton University, Princeton, NJ 08544, USA

ARTICLE INFO

Article history:
Received 12 May 2011
Received in revised form 1 August 2011
Accepted 8 August 2011
Available online 16 August 2011

Keywords:
Nanoparticles
Cyclosporine A
Mannitol
Pulmonary drug delivery
Dry powder aerosol
Dissolution

ABSTRACT

This study aims to improve the dissolution of inhalable cyclosporine A nanoparticles by formulating the drug with mannitol as a hydrophilic nano-matrix former. The effect of mannitol content on the aerosol performance of the nano-matrix particles was also examined. Cyclosporine A nanosuspensions were produced by anti-solvent precipitation using a multi-inlet vortex mixer. Various amounts of mannitol were dissolved into the suspensions before spray drying to obtain micron-sized aggregates (nano-matrix powders). Dissolution properties of the powders in an aqueous medium, with the drug content, aggregate size distribution, surface roughness, physicochemical properties and aerosol performance were determined. The powders contained amorphous cyclosporine A and α-crystalline mannitol, with drug content being very close to the theoretical doses. Inclusion of mannitol enhanced the dissolution rate of the drug, without significantly affecting the aggregate size distribution, surface roughness and aerosol performance. This formulation approach may be applicable to improving the dissolution rate and bioavailability of hydrophobic drugs.

1. Introduction

Inhalation is by far the best route of administration for drugs to treat respiratory diseases such as asthma, chronic obstructive pulmonary disease and cystic fibrosis. It directly targets the site of action and reduces the dosage and systemic adverse effects. The aerodynamic diameter of the drug particles should be <5 μm for optimal airway deposition. However, particles in this size range have high specific surface areas. Hence they are generally cohesive and tend to disperse poorly.

Inter-particulate cohesion can be reduced by using rough particles. Small increases in the surface roughness of bovine serum albumin (BSA) particles were shown to significantly improve aerosol performance (Adi et al., 2008c; Chew and Chan, 2001a; Chew et al., 2005). These corrugated particles were produced by spray drying aqueous protein solutions. However, the use of solutions is limited, as it depends on the solubility of the drugs and the nature of the solvent. Furthermore, since the drying is fast (in the order of seconds), the resulting surface roughness of the particles is difficult to be controlled.

A novel method to control surface roughness is by spray drying nanosuspensions to obtain micron-sized aggregates, which are called nano-matrix particles (Kwok et al., 2011). Surface roughness was modified by varying the size of the primary nanoparticles. The resultant nano-matrix particles were less cohesive than smooth particles and showed excellent aerosol performance (Kwok et al., 2011). Besides improving aerosolisation, nano-matrix particles may enhance the dissolution and, consequently, the bioavailability of drugs with low aqueous solubility. The large specific surface area of nano-matrix particles promotes exposure of the drug to the surrounding liquid medium, such as water or lung fluid. To maximise favourable conditions for dissolution, a hydrophilic excipient may be incorporated into the nano-matrix by dissolving in the nanosuspension prior to spray drying. This excipient would then become a continuous matrix former in the nano-matrix particles and attract water upon contact with aqueous media for improved dissolution.

In the present study, we used cyclosporine A as the model hydrophobic drug. It is a cyclic peptide (molecular weight 1202.6 Da), being practically insoluble in water but freely soluble in organic solvents such as ethanol, methanol, acetone, chloroform, ether and methylene chloride (Merck Index, 2011). It is a potent immunosuppressant usually administered orally or intravenously for the prevention of organ transplant rejection (Martindale: The

* Corresponding author. Tel.: +61 2 9351 3054; fax: +61 2 9351 4391.
** Corresponding author. Tel.: +81 96 326 4078; fax: +81 96 326 5048.
E-mail addresses: kcyama@ph.sojo-u.ac.jp (K. Yamasaki), kim.chan@sydney.edu.au, kimc@pharm.usyd.edu.au (H.-K. Chan).

0378-5173/$ – see front matter © 2011 Elsevier B.V. All rights reserved.
doi:10.1016/j.ijpharm.2011.08.010

Complete Drug Reference, 2011). In the case of lung transplantation, inhaled cyclosporine A is more preferable than systemic delivery as the toxic side effects and dosage may be minimised. Nebulised cyclosporine A has been shown to be effective in human lung transplant recipients. The nebule solvents employed in the clinical trials were ethanol (Iacono et al., 1996; O'Riordan et al., 1995) and propylene glycol (Corcoran et al., 2004; Groves et al., 2010; Iacono et al., 2004, 2006, 1997). As both of these solvents are potential irritants (Martindale: The Complete Drug Reference, 2011), alternative formulations have been attempted. These included hydrofluoroalkane-based solution metered dose inhalers with ethanol as a co-solvent (Myrdal et al., 2004), spray dried powder from a 95% ethanolic solution (Lechuga-Ballesteros et al., 2003) and large porous particles (median volume diameter 7 μm, particle density 0.2 g/cm^3) produced by co-spray freeze drying with inulin from a *tert*-butyl alcohol/water co-solvent solution (Zijlstra et al., 2007). Although the large porous particles showed good aerosol performance (50% fine particle fraction at 60 L/min) and enhanced dissolution profiles, the drug loading was relatively low (10–50% w/w cyclosporine A) (Zijlstra et al., 2007). Furthermore, inulin has not been approved for inhalation and spray freeze drying is a slow process. In fact, the drying of the frozen cyclosporine A/inulin droplets took 48 h (Zijlstra et al., 2007). Thus, a more efficient particle production method was warranted. Micron-sized aggregates of cyclosporine A nanoparticles with high drug loading could be formulated by anti-solvent precipitation and spray drying (Chiou et al., 2008). The procedures were fast and could be precisely controlled. The spray dried aggregates were essentially nano-matrix particles, although this term was not used in the paper. The powders dispersed well (54% fine particle fraction at 60 L/min) and the aggregates appeared to dissociate upon contact with water (Chiou et al., 2008) but there was no quantitative data on the dissolution rate.

The current study aimed to further explore the cyclosporine A nano-matrix formulation by incorporating mannitol as a hydrophilic matrix former. Our objectives were:

i) To increase the dissolution rate of cyclosporine A nano-matrix particles in aqueous medium and;
ii) To investigate the effect of mannitol content on the aerosol performance of the nano-matrix particles.

Mannitol was chosen as the matrix former because spray dried mannitol is crystalline, stable and has recently been approved by regulatory authorities for inhalation use in Australia, a number of Asian and European Union countries and the USA (Pharmaxis, 2009, 2010).

2. Materials and methods

2.1. Materials

Cyclosporine A was purchased from Fujian Kerui Pharmaceutical Co. Ltd., Fujian, China, refrigerated until use; Emultop® soy bean lecithin from Cargill Texturizing Solutions, MN, USA, frozen until use; Lactochem® α-lactose monohydrate from Friesland-Campina Domo, Amersfoort, The Netherlands; Pearlitol® 160C mannitol from Rocquette, Lestrem, France; absolute undenatured ethanol, chromatographic grade methanol and Terumo® 20 mL syringes (internal diameter 20.15 mm) from Lomb Scientific, NSW, Australia; phosphoric acid from MP Biomedicals, OH, USA; Myrj 52 (polyoxyethylene 40 stearate) from Sigma–Aldrich, NSW, Australia; potassium dihydrogen phosphate from Biolab, VIC, Australia; and sodium hydroxide from VMR International, Dorset, UK. Deionised water (electrical resistivity > 2 MΩ cm at 25 °C) was obtained from a Modulab Type II Deionisation System (Continental Water Systems, NSW, Australia).

2.2. Preparation of nano-matrix particles

The production conditions were adapted from a previous study (Chiou et al., 2008). The primary nanoparticles of cyclosporine A were obtained by anti-solvent precipitation using a four-stream multi-inlet vortex mixer (MIVM). Details on the design and applications of the MIVM have been described elsewhere (Akbulut et al., 2008; Gindy et al., 2008; Liu et al., 2008a,b; Russ et al., 2010). Briefly, the mixer consists of four inlets through which liquid reactants were pumped at controlled flow rates. Subsequently, micro-mixing of the liquids and particle precipitation occurred inside the mixing chamber and the resultant suspension was collected at the outlet.

The MIVM setup is shown schematically in Fig. 1. Two syringe pumps (Model PHD 2000, Harvard Apparatus, MA, USA) were used to control the flow rate and volume of liquid streams from four syringes (i.e. two syringes per pump). Cyclosporine A was dissolved in absolute ethanol at a concentration of 50 mg/mL (Solution I). Lecithin and lactose as nanoparticle stabilisers were dissolved together in water at 0.0125% (w/v) and 0.5% (w/v), respectively (Solution II). Solution I was loaded into two syringes, with about 21 mL in each syringe. Likewise, Solution II was loaded into two other syringes to the same volume. All four syringes were connected to the MIVM (Fig. 1) with each syringe dispensing 20 mL at 30 mL/min. The product from the mixer outlet was collected in a 600 mL beaker containing 400 mL deionised water stirred with a magnetic bar (39 mm long, 8 mm diameter) at 650 rpm. The suspension was divided into two equal portions by mass. Each portion was separately used to make one batch of nano-matrix particles. Therefore, one precipitation run could produce two batches of nano-matrix particles. Mannitol was dissolved into the suspension batches. Four cyclosporine A-to-mannitol mass ratios were investigated, namely 1:0, 1:0.25, 1:0.5 and 1:1. The corresponding amounts of mannitol added to achieve the ratios were 0, 0.25, 0.5 and 1.0 g, respectively. After dissolving the mannitol, the nanoparticles in suspension were sized by dynamic light scattering (see below). The suspensions were then refrigerated for at least 2 h before spray drying.

Each suspension was spray dried using a laboratory-scale spray dryer (Mini Spray Dryer B-290, Büchi Labortechnik, Flawil, Switzerland) coupled to a Büchi Dehumidifier B-296 in open-loop suction mode under the following conditions: inlet temperature of 120 °C, outlet temperatures of 46–59 °C, aspiration rate of 100% (i.e. 38 m^3/h), compressed air atomisation flow rate set at 65 mm on the rotameter (i.e. 819 NL/h) and liquid feed rate of 10% (i.e. 3.5 mL/min). The spray dried powders were stored at 22 °C in desiccators with silica gel. The nano-matrix particles were labelled as A, B, C and D, with increasing amounts of mannitol.

2.3. Dynamic light scattering

The nanoparticles in suspension were sized by dynamic light scattering (Malvern Zetasizer Nano ZS; Malvern, Worcestershire, UK) before spray drying. The measurement parameters were as follows: the particle and dispersant refractive indices were 1.578 and 1.338, respectively, the absorption value of cyclosporine A was 0.1 and the dispersant viscosity was 1.3617 mPa s. The samples were measured in a quartz cuvette at 20 °C. Particle size distributions were measured in triplicate ($n = 3$).

2.4. Drug content determination

Two milligrams of the spray dried powder was dissolved in 25 mL ethanol/water solution (50/50% v/v). The cyclosporine

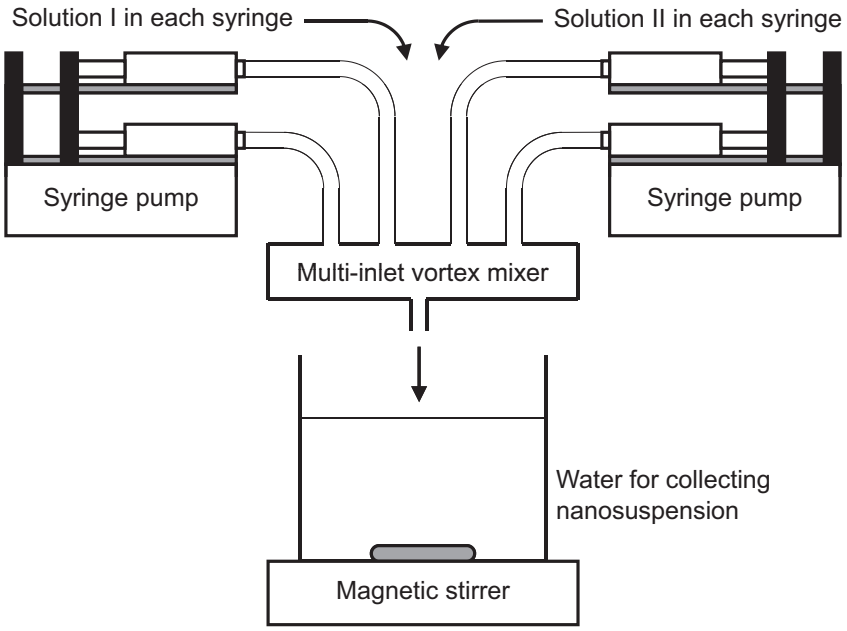

Fig. 1. Schematics of the MIVM setup. Diagram not drawn to scale.

A content was then assayed by high performance liquid chromatography (HPLC). The HPLC system comprised of a Shimadzu CBM-20A controller, LC-20AT pump, SIL-20A HT autosampler, SPD-20A UV/VIS detector and LCsolution Version 1.24 SP1 control and analysis software (Shimadzu Corporation, Kyoto, Japan). The column was Alltima C18 (5 μm particle size, 4.6 mm × 250 mm; Alltech Associates, IL, USA) and kept at 70 °C by a Waters Temperature Control Module and oven (Waters Corporation, MA, USA). The mobile phase was composed of acetonitrile, water, methanol and phosphoric acid in 360/50/90/2.5 volumetric ratios and was filtered through a Magna nylon filter membrane (pore size 0.45 μm; GE Water and Process Technologies, PA, USA) before use. The mobile phase flow rate was 1.5 mL/min, injection volume 50 μL and detection wavelength 210 nm. Each powder was tested in triplicate ($n = 3$). The assayed cyclosporine A content was compared against the theoretical dose, which was calculated from the masses of ingredients used in the formulations (Table 1).

2.5. Scanning electron microscopy

The surface morphology of the nano-matrix particles was observed by field emission scanning electron microscopy (SEM) at 2.0 kV (Zeiss Ultra Plus; Carl Zeiss SMT AG, Oberkochen, Germany). The powders were sprinkled onto carbon sticky tape mounted on SEM stubs and sputter coated with approximately 11.3 nm palladium/gold using a K550X sputter coater (Quorum Emitech, Kent, UK) before imaging.

2.6. Laser diffraction

Volume size distributions of the nano-matrix particles were determined by laser diffraction on a Mastersizer 2000 laser diffractometer (Malvern Instruments, Worcestershire, UK). The powders were dispersed through the laser measurement zone from 0.5 to 4 bar of pressure by a Scirocco 2000 dry powder feeder (Malvern Instruments, Worcestershire, UK). The particle refractive index and absorption were 1.578 and 0.1, respectively. The dispersant refractive index was 1.000 for air. The measurements were done in triplicate ($n = 3$). The size data were expressed as $D_{0.1}$, $D_{0.5}$, $D_{0.9}$, which are equivalent spherical volume diameters at 10%, 50% and 90% cumulative volume, respectively.

2.7. Thermogravimetric analysis

Thermogravimetric analysis (TGA) was conducted on a thermogravimetric analyser (Model 2050; TA Instruments, DE, USA) to determine the residual solvent content in the spray dried powders. Each sample (3 ± 1 mg) was loaded onto an open platinum pan and the mass measured under 90 cm^3/min nitrogen purge from 20 to 120 °C at a heating rate of 10 °C/min.

2.8. Differential scanning calorimetry

Differential scanning calorimetry (DSC) was performed on the nano-matrix particles, raw cyclosporine A, raw mannitol and a 1:1 (w/w) physical mixture of raw cyclosporine A and raw mannitol using a differential scanning calorimeter (Model 821e; Mettler

Table 1
Composition of the nano-matrix particles. Assayed cyclosporine A (CsA) contents expressed as mean ± standard deviation ($n = 3$).

Formulation	Content (% w/w)					Percentage of theoretical CsA content assayed
	Theoretical				Assayed	
	CsA	Lactose	Lecithin	Mannitol	CsA	
A	91.1	8.7	0.2	0.00	89.5 ± 0.7	98.2 ± 0.7
B	74.2	7.1	0.2	18.6	74.3 ± 0.6	100.1 ± 0.8
C	62.6	6.0	0.2	31.3	62.1 ± 0.5	99.1 ± 0.8
D	47.7	4.5	0.1	47.7	47.3 ± 0.3	99.3 ± 0.7

Toledo, Greigensee, Switzerland). Each sample (3 ± 1 mg) was weighed into a 40 μL aluminium crucible with a vent hole in the lid and heated from 20 to 400 °C at a heating rate of 10 °C/min under 250 cm^3/min nitrogen purge.

2.9. X-ray diffraction

X-ray diffraction (XRD) was carried out under ambient conditions using an X-ray diffractometer (Model D5000; Siemens, Munich, Germany) to analyse the crystallinity of the powders. Cu Kα radiation at 30 mA and 40 kV was applied with an angular increment of 0.04° at 2 s per step covering a 2θ range of 5–40°.

2.10. Atomic force microscopy

Particle surface roughness was quantified using atomic force microscopy (AFM) (Multimode Model MMAFMLN with Nanoscope IIIa controller, Veeco Metrology, CA, USA). The samples were sprinkled onto carbon sticky tabs and imaged at a scan rate of 0.5 Hz using Tap300Al-G cantilevers (BudgetSensors, Sofia, Bulgaria) in tapping mode. Areas of 500 nm × 500 nm on the nano-matrix particles were imaged with 512 × 512 sample points. The root mean square (RMS) roughness was obtained over the entire scanned area for six individual particles (n = 6).

2.11. In vitro aerosol performance

The aerosol performance was assessed by dispersing 5 mg of powder into a next generation impactor (NGI) under two conditions: (i) from a Rotahaler® (Allen & Hanburys, Boronia, VIC, Australia) at 60 L/min of air flow for 4 s, as the low dispersion condition; and (ii) from an Aerolizer® at 100 L/min for 2.4 s, as the high dispersion condition. The Rotahaler® and Aerolizer® are single-dose commercial devices for proprietary inhalation formulations, with specific air flow resistances of 0.04 and 0.07 $cmH_2O^{0.5}$/(L/min), respectively (Clark and Hollingworth, 1993; Molimard et al., 2007). The mean FPF of the commercial product Rotacaps® 400 generated from a Rotahaler® at 60 L/min was lower than that from a Cyclohaler® (another tradename for the Aerolizer®) at 90 L/min (Srichana et al., 1998). The mean peak inhaled flow rates generated by human subjects through the Cyclohaler® in a scintigraphic study were about 100 L/min (Pitcairn et al., 1997). This value is also consistent with an *in vitro* study, which noted that 105 L/min could be generated through the Aerolizer® at a comfortable inspiratory effort (Chew and Chan, 2001b). This was the purpose for using the Rotahaler® at 60 L/min and the Aerolizer® at 100 L/min in the present study to represent a low and a high dispersion condition, respectively.

Size 3 hydroxypropyl methylcellulose (Capsugel, West Ryde, NSW, Australia) were used for powder loading for both inhalers. One capsule was tested per run. Three runs were conducted for each powder under both dispersion conditions (n = 3). To minimise particle bounce, the impactor stages were coated with silicon grease (Slipicone; DC Products, Waverley, VIC, Australia) before testing. Critical air flow was achieved in the dispersion setup, as the ratio of the absolute pressures after the flow control valve to that before was less than 0.5 (British Pharmacopoeia, 2011). After dispersion, the powder deposits on each inhaler and NGI part was exhaustively washed with 5 mL methanol/water solution (volumetric ratio 85/15) except for Stage 1, which was washed with 15 mL of the same solution. The HPLC conditions for the assay were identical to those for drug content determination. The cut-off diameters of the NGI stages at 100 L/min were calculated with the adjustment equations given in Appendix XII C of British Pharmacopoeia (2011). The emitted fraction (EF) was the total amount of powder that exited the inhaler with respect to the recovered dose. The fine particle fraction (FPF) was defined as the mass fraction of particles <5.0 μm with respect to the recovered dose. At 60 and 100 L/min, the upper aerodynamic cutoff diameters of Stages 2 and 3 are 8.06 and 4.46 μm and 6.12 and 3.42 μm, respectively. The cumulative mass fraction <5.0 μm (i.e. the FPF) was obtained by interpolation between the two cumulative mass fractions corresponding to the cutoff diameters for Stages 2 and 3 at the respective flow rate.

2.12. Dissolution rate measurement

Two hundred millilitres of dissolution medium (phosphate buffer pH 7.4 BP with 0.25% (w/v) Myrj 52) maintained at 37 ± 0.5 °C in a 250 mL glass beaker was passed through a 25 mm flow-through filter holder (Sartorius Stedim Biotech, Göttingen, Germany) containing a HT Tuffryn® 0.2 μm pore size polysulfone filter membrane disc (Pall Corporation, NY, USA) and an amount of powder with a theoretical dose of 1 mg of cyclosporine A. The appropriate sample mass was calculated from the theoretical cyclosporine A content (Table 1). One milligram of raw cyclosporine A was also tested as a control. The dose of 1 mg of cyclosporine A would achieve a maximum concentration of 5 μg/mL in 200 mL of dissolution medium. This met sink conditions because the saturated concentration of cyclosporine A in the dissolution medium at 37 °C was measured to be 215 μg/mL on the nano-matrix powders in preliminary solubility tests. An excess amount of raw cyclosporine A or nano-matrix particles in 200 mL of dissolution medium at 37 °C was stirred by a magnetic bar (29 mm long, 6 mm diameter) at 400 rpm for two days. Samples filtered through an Anotop® 10 pore size 0.02 μm syringe filter (Whatman, Kent, UK) were taken to assay the saturated concentration. The phosphate buffer was prepared by adding 250 mL of 0.2 M potassium dihydrogen phosphate solution to 393.4 mL of 0.1 M sodium hydroxide solution (British Pharmacopoeia, 2011). The dissolution medium was recirculated in a closed-loop configuration at 1.5 mL/min by a peristaltic pump (Model Minipuls 3, Gilson, WI, USA). New Tygon® R-3603 tubings (Saint-Gobain Performance Plastics, Courbevoie, France) were used to connect the various parts of the setup for each run. The dissolution medium in the beaker was stirred with a magnetic bar (29 mm long, 6 mm diameter) at 400 rpm. At specific time intervals, 0.7 mL samples were withdrawn from the beaker, filtered through an Anotop® 10 pore size 0.02 μm syringe filter and collected in HPLC vials for assay. To maintain the total liquid volume in the setup, 0.7 mL of fresh dissolution medium was immediately added to the beaker for recirculation after each sampling. The measurement was conducted for 120 min. The HPLC conditions for the assay were identical to those for drug content determination. Three dissolution tests were conducted for each powder (n = 3).

2.13. Statistical data analysis

The data were analysed statistically using one-way analysis of variance (ANOVA), followed by Tukey multiple comparisons post hoc test to evaluate differences between the means. All statistical procedures were performed with StatMate III (ATMS, Tokyo, Japan) statistical software. Differences with $p > 0.05$ were deemed to be statistically non-significant.

3. Results and discussion

The MIVM method produced stable nanosuspensions. The *Z*-average diameters of formulation A–D measured by dynamic light scattering intensity before spray drying were 225.7 ± 4.9, 255.0 ± 25.1, 256.0 ± 3.6 and 294.7 ± 1.2 nm (mean ± standard deviation), respectively. Since agglomeration is very common for nanoparticles in suspension, the data implied a slight increase in the

agglomerate and/or primary particle sizes with increasing mannitol concentration.

Nano-matrix particles were successfully produced from all four formulations. The assayed cyclosporine A contents in the spray dried powders were very close to the theoretical doses (Table 1). Thus no cyclosporine A was lost in the production process. The primary nanoparticles were visible from the SEM images and were generally 200–300 nm in diameter (Fig. 2), which conformed

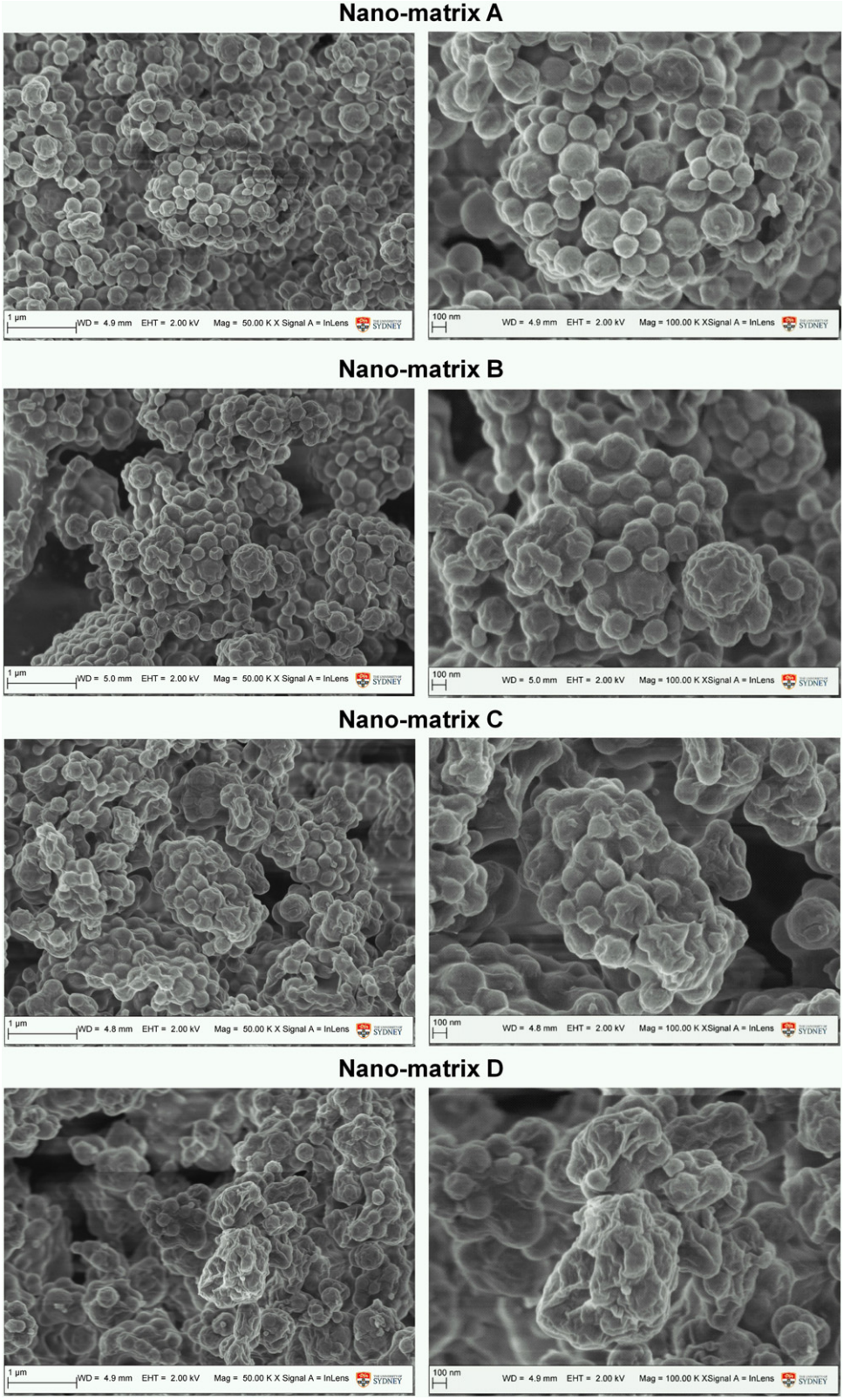

Fig. 2. SEM images of cyclosporine A–mannitol nano-matrix particles. For each formulation, images at 50,000× and 100,000× magnification are on the left and right, respectively.

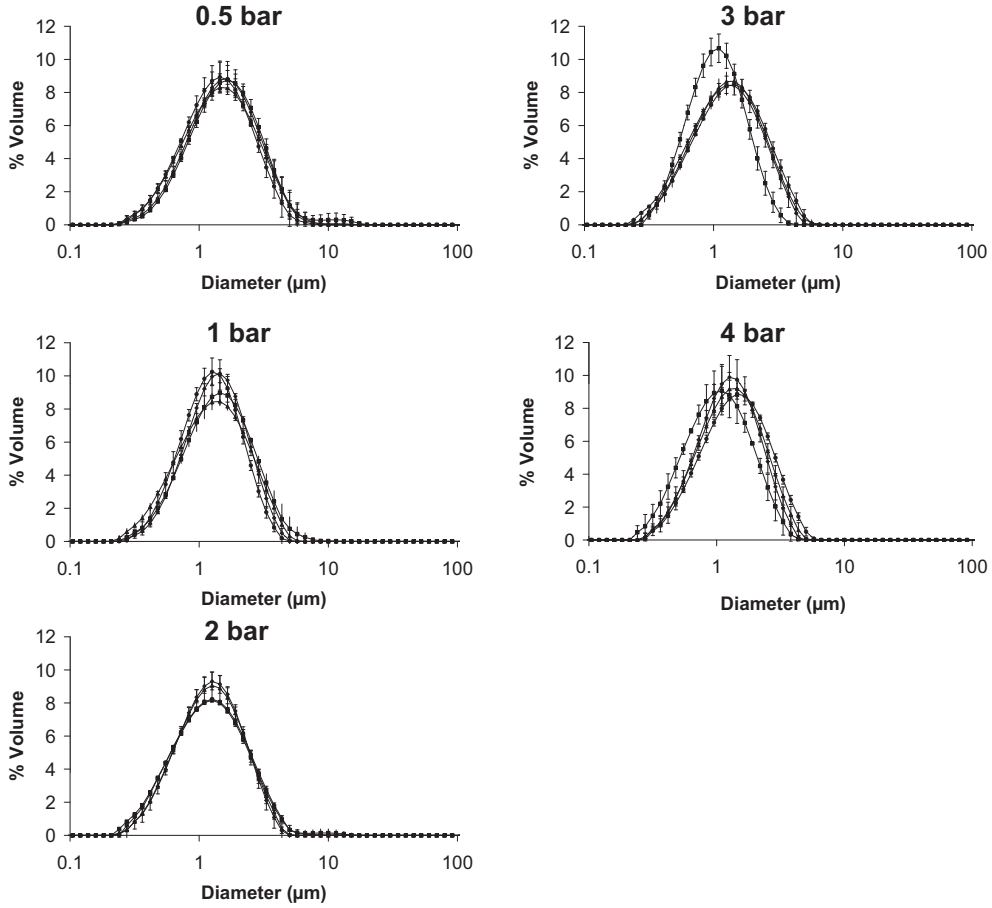

Fig. 3. Laser diffraction size distributions of nano-matrix particles at various dispersion pressures. Data presented as mean ± standard deviation ($n = 3$). (■ Nano-matrix A, ♦ nano-matrix B, ▲ nano-matrix C, ● nano-matrix D). Data presented as mean ± standard deviation ($n = 3$). Statistically significant differences between the $D_{0.5}$ of nano-matrix particles at 0.5 bar include A and C ($p < 0.05$), A and D ($p < 0.01$) and B and D ($p < 0.05$). At 4 bar, all pairs of data were statistically significant from each other ($p < 0.05$) except for B and C ($p > 0.05$).

to the dynamic light scattering data. The primary nanoparticles became less distinct and appeared to be embedded in a web or coating with increasing mannitol content. The coating is believed to be mannitol. As the droplets shrunk during spray drying, the nanoparticles clustered together to form the micron-sized aggregates. Simultaneously, mannitol came out of solution and formed a continuous deposit amongst the nanoparticles. Further evidence for the embedding of the nanoparticles in a mannitol matrix is provided by TGA results. The measured solvent contents of nano-matrix A–D were 2.32%, 1.05%, 1.44% and 1.00% (w/w), respectively. The reduced solvent content of the mannitol-containing nano-matrix particles was attributed to the non-hygroscopic nature of this excipient (Rowe et al., 2011).

Since the spray drying conditions were the same for all four formulations, the nano-matrix particles produced were comparable in size. The size distributions at the five dispersion pressures are shown in Fig. 3. Although the overall particle size distributions were seemingly stable across the dispersion pressures from these plots, the $D_{0.5}$ varied with the formulation and dispersion pressure (Fig. 4). At the lowest pressure (0.5 bar), $D_{0.5}$ significantly decreased with increasing mannitol content. This trend was inversed with increasing dispersion pressure. The pressure of 2 bar was the turning point of this inversion, at which a $D_{0.5}$ of 1.1 μm was achieved for all formulations. The continual reduction in $D_{0.5}$ for the nano-matrix A may be due to fragmentation of the aggregates at high pressures. The small amount of mannitol in nano-matrix B might have prevented fragmentation by holding the nanoparticles together. Thus its $D_{0.5}$ reached a plateau beyond 2 bar. The data of nano-matrix particles C and D suggest that the nano-matrix particles with increasing mannitol content mechanically strengthened the aggregates and reduced their tendency to fracture. They also formed larger aggregates (e.g. super-aggregates formed from multiple nano-matrix particles) at high pressures but the exact mechanism for this is unclear.

The DSC and XRD results are shown in Figs. 5 and 6, respectively. The small endothermic peak of raw cyclosporine A and the physical mixture at 130 °C was due to dehydration (Fig. 5). This

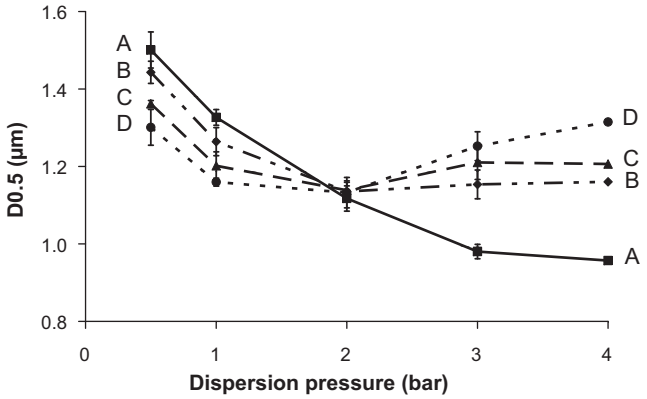

Fig. 4. The median volume diameter of nano-matrix particles at various dispersion pressures measured by laser diffraction. A–D denote plots of the respective nano-matrix formulation. Data presented as mean ± standard deviation ($n = 3$).

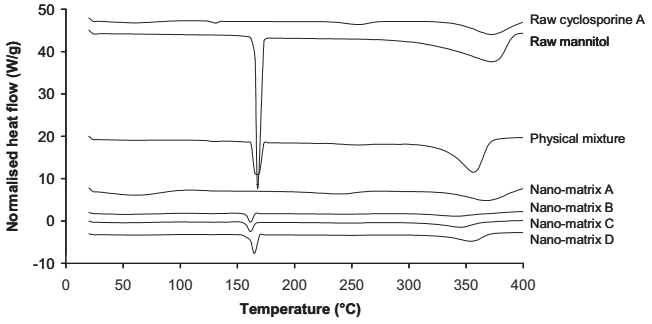

Fig. 5. DSC curves of raw cyclosporine A, raw mannitol, a 1:1 (w/w) physical mixture of raw cyclosporine A and raw mannitol and nano-matrix particles A–D.

peak was absent in the spray dried powders. Mannitol showed a large endothermic melting peak at 170 °C. In the nano-matrix particles, this peak was shifted slightly to a lower temperature and increased in size with mannitol content. The mannitol melting enthalpy with respect to the powder mass for nano-matrix particles B–D were 53.46, 94.70 and 135.85 J/g, respectively. The XRD data showed that both raw and nano-matrix cyclosporine A were amorphous, whereas raw mannitol was the crystalline β-form (Fig. 6). The diffraction pattern of the physical mixture was essentially a summation of the patterns of the raw ingredients. On the other hand, the nano-matrix particles were partially amorphous and contained α-crystalline mannitol, with diffraction peaks increasing in prominence with mannitol content (Fig. 6). A previous study demonstrated that while β-mannitol was obtained when spray dried alone, the α-form was produced when co-spray dried with a corticosteroid and a long-acting β_2-agonist from solution (Kumon et al., 2010). Those co-spray dried formulations contained about 90% (w/w) mannitol. In the present nano-matrix study, the mannitol content was lower and it was co-spray dried with nanoparticles rather than dissolved drugs. Both the previous and present studies employed ethanol/water co-solvent mixtures in various volumetric proportions. This suggests that, at least for ethanol/water co-solvent systems, mannitol preferably crystallises in the α-form when co-spray dried with other compounds, whether those compounds are initially present as molecules in solution or suspended nanoparticles.

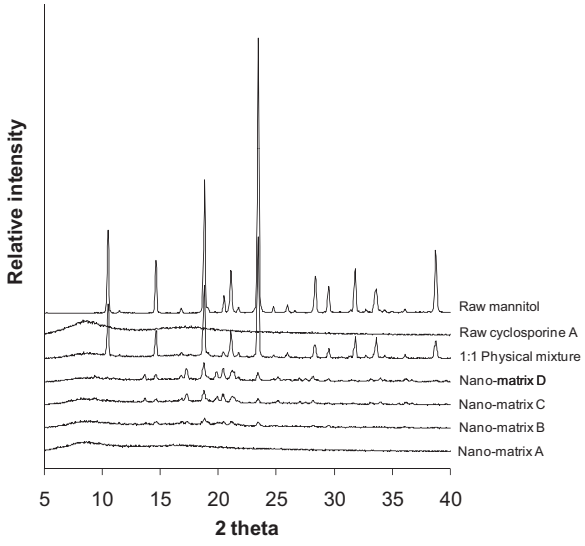

Fig. 6. XRD patterns of raw cyclosporine A, raw mannitol, a 1:1 (w/w) physical mixture of raw cyclosporine A and raw mannitol and nano-matrix particles A–D.

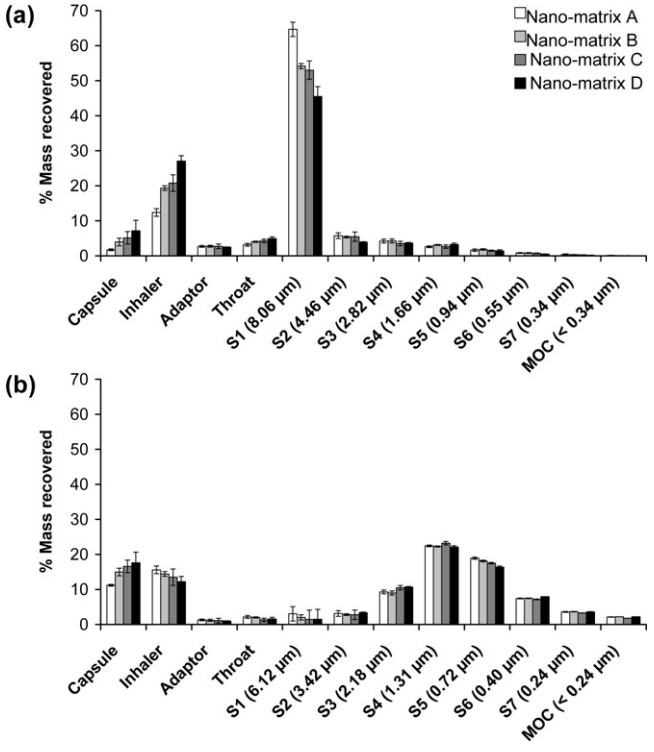

Fig. 7. Dispersion data of nano-matrix particles using (a) the Rotahaler® at 60 L/min and (b) the Aerolizer® at 100 L/min. Data presented as mean ± standard deviation ($n = 3$). S1–S7 denote impactor stages 1–7, followed by their corresponding lower aerodynamic cutoff diameter in parentheses. MOC is the NGI micro-orifice collector.

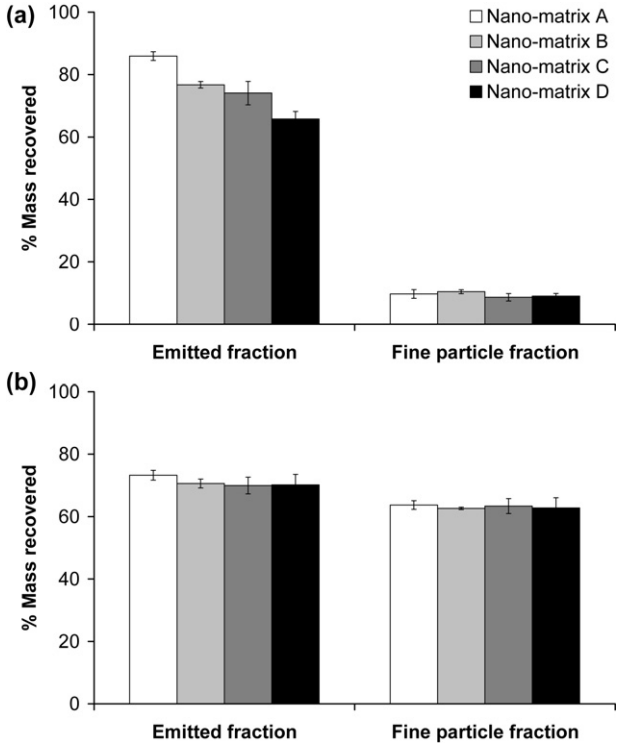

Fig. 8. EF and FPF of nano-matrix particles under (a) the Rotahaler® at 60 L/min and (b) the Aerolizer® at 100 L/min. Data presented as mean ± standard deviation ($n = 3$). Statistically significant differences between the EFs of nano-matrix particles from the Rotahaler® include A and B ($p < 0.01$), A and C ($p < 0.01$), A and D ($p < 0.001$), B and D ($p < 0.01$) and C and D ($p < 0.05$). No statistically significant differences were found amongst the FPFs of Rotahaler® and the EFs and FPFs of Aerolizer®.

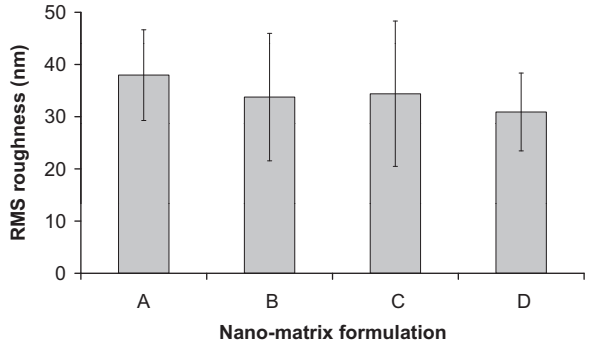

Fig. 9. RMS roughness of nano-matrix particles measured by AFM. Data presented as mean ± standard deviation ($n = 6$). The means were not statistically significant ($p > 0.05$).

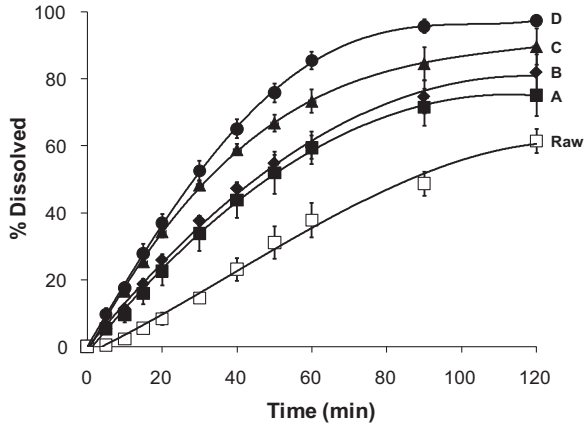

Fig. 10. Dissolution profiles of raw cyclosporine A and nano-matrix particles (□ raw cyclosporine A, ■ nano-matrix A, ♦ nano-matrix B, ▲ nano-matrix C, ● nano-matrix D). Data presented as mean ± standard error ($n = 3$). After 30 min, nano-matrix particles A and C, A and D and B and D were significantly different ($p < 0.05$), all four nano-matrix particles were significantly different to raw cyclosporine A ($p < 0.01$). After 60 min, nano-matrix particles A and D, B and D were significantly different ($p < 0.01$), all four nano-matrix particles were significantly different to raw cyclosporine A ($p < 0.05$). After 120 min, nano-matrix particles A and D were significantly different ($p < 0.05$), both C and D were significantly different to raw cyclosporine A ($p < 0.01$).

The aerosol performance results are shown in Figs. 7 and 8. As expected, the powders performed poorly under the low dispersion condition, with FPFs of only 10% (Fig. 8a). This was due to high deposition on Stage 1 (cutoff diameter = 8.06 μm), implying the presence of large agglomerates in the aerosol (Fig. 7a). Deposition on the upper stages was greatly reduced and FPFs of 60% could be achieved under the high dispersion condition (Fig. 8b). Increasing the mannitol content increased capsule and inhaler deposition but decreased Stage 1 deposition and EF under the low dispersion condition (Figs. 7a and 8a). On the other hand, inhaler and Stage 1 deposition decreased with mannitol content under the high dispersion condition, although the differences were not statistically significant (Fig. 7b). However, these changes in deposition did not affect the FPFs under either dispersion condition (Fig. 8). The EFs of nano-matrix particles A–C dispersed from the Aerolizer® were lower than those from the Rotahaler® (Fig. 8), despite the higher air flow rate used with the Aerolizer®. This was mainly due to the higher capsule retention in the Aerolizer® (Fig. 7), which could be attributed to differences in the construction and mode of use between the two inhalers. For the Rotahaler®, the capsule was twisted open inside the inhaler prior to dispersion. The opened halves of the capsule consequently provided large exits for the powder. On the other hand, the capsule in the Aerolizer® was pierced by four metal pins at each end. The total area of the pierced holes was much less than that of the opened capsule in the Rotahaler®, leading to poorer capsule emptying hence lower EFs in the Aerolizer®.

It is well known that surface roughness improves powder dispersion (Adi et al., 2008a,c; Chew and Chan, 2001a; Chew et al., 2005; Kwok et al., 2011). Since nano-matrix particles are aggregates of nanoparticles, their surfaces are invariably rough (Kwok et al., 2011). From the SEM images, the cyclosporine A nano-matrix particle surface became smoother with mannitol content (Fig. 2). However, AFM measurements showed no statistically significant difference in the mean RMS roughness between the four cyclosporine A nano-matrix formulations, despite a slight reduction in the mean values with increasing mannitol content (Fig. 9). The lack of difference in surface roughness may explain the similarity in the FPFs (Fig. 8). In view of the variability in the RMS roughness data, the AFM measurements may be improved by performing more replicates or by using a high-aspect-ratio tip for higher image resolution. A non-contact optical technique such as scanning white-light profilometry may also be useful to quantify nano-scale surface roughness (Adi et al., 2008b).

Mannitol was incorporated as a matrix former to improve the dissolution rate of the hydrophobic cyclosporine A nanoparticles. To compare the dissolution rate of the nano-matrix formulations, the testing method must be able to overcome wetting problems and differentiate the dissolution rates of poorly water-soluble powders. The flow-through setup fulfils these criteria and has been shown to be the best technique for hydrophobic nanoparticles (Heng et al., 2008). Thus this method was chosen for the current study. The results showed that formulating cyclosporine A as nano-matrix particles greatly improved dissolution compared to the raw powder (Fig. 10). In addition, the use of mannitol as a hydrophilic matrix former further enhanced the dissolution rate, with the amount of cyclosporine A dissolved after 2 h significantly increased from 75% (nano-matrix A) to 100% (nano-matrix D) (Fig. 10). Therefore mannitol acted as a dissolution enhancer without affecting the aerosol performance of the nano-matrix particles. This is potentially useful in improving the bioavailability of inhaled cyclosporine A. The formulation technique demonstrated in this study may be applied to other hydrophobic drugs for pulmonary delivery. *In vivo* pharmacokinetic studies are ultimately required to evaluate its clinical value.

4. Conclusion

Cyclosporine A nano-matrix particles with various amounts of mannitol were successfully produced by anti-solvent precipitation followed by spray drying. The nano-matrix particles were partially amorphous (due to the cyclosporine A), with the mannitol component being in the crystalline α-form. Incorporation of mannitol as a hydrophilic matrix former improved the dissolution rate, without significantly affecting the aggregate size distribution, surface roughness and aerosol performance. This formulation technique may potentially enhance the bioavailability of inhaled cyclosporine A or other hydrophobic drugs.

Acknowledgement

This work was financially supported by the Australian Research Council (Discovery Project 0985367).

References

Adi, H., Traini, D., Chan, H.-K., Young, P.M., 2008a. The influence of drug morphology on the aerosolisation efficiency of dry powder inhaler formulations. J. Pharm. Sci. 97, 2780–2788.

Adi, S., Adi, H., Chan, H.-K., Young, P.M., Traini, D., Yang, R., Yu, A., 2008b. Scanning white-light interferometry as a novel technique to quantify the surface roughness of micron-sized particles for inhalation. Langmuir 24, 11307–11312.
Adi, S., Adi, H., Tang, P., Traini, D., Chan, H.-K., Young, P.M., 2008c. Micro-particle corrugation, adhesion and inhalation aerosol efficiency. Eur. J. Pharm. Sci. 35, 12–18.
Akbulut, M., Reddy, N.K., Bechtloff, B., Koltzenburg, S., Vermant, J., Prud'homme, R.K., 2008. Flow-induced conformational changes in gelatin structure and colloidal stabilization. Langmuir 24, 9636–9641.
British Pharmacopoeia, 2011. Spottiswoode, London.
Chew, N.Y.K., Chan, H.-K., 2001a. Use of solid corrugated particles enhance powder aerosol performance. Pharm. Res. 18, 1570–1577.
Chew, N.Y.K., Chan, H.-K., 2001b. In vitro aerosol performance and dose uniformity between the Foradile® Aerolizer® and the Oxis® Turbuhaler®. J. Aerosol Med. 14, 495–501.
Chew, N.Y.K., Tang, P., Chan, H.-K., Raper, J.A., 2005. How much particle surface corrugation is sufficient to improve aerosol performance of powders? Pharm. Res. 22, 148–152.
Chiou, H., Chan, H.-K., Heng, D., Prud'homme, R.K., Raper, J.A., 2008. A novel production method for inhalable cyclosporine A powders by confined liquid impinging jet precipitation. J. Aerosol Sci. 39, 500–509.
Clark, A.R., Hollingworth, A.M., 1993. The relationship between powder inhaler resistance and peak inspiratory conditions in healthy volunteers—implications for in vitro testing. J. Aerosol Med. 6, 99–110.
Corcoran, T.E., Smaldone, G.C., Dauber, J.H., Smith, D.A., McCurry, K.R., Burckart, G.J., Zeevi, A., Griffith, B.P., Iacono, A.T., 2004. Preservation of post-transplant lung function with aerosol cyclosporin. Eur. Respir. J. 23, 378–383.
Gindy, M.E., Panagiotopoulos, A.Z., Prud'homme, R.K., 2008. Composite block copolymer stabilized nanoparticles: simultaneous encapsulation of organic actives and inorganic nanostructures. Langmuir 24, 83–90.
Groves, S., Galazka, M., Johnson, B., Corcoran, T., Verceles, A., Britt, E., Todd, N., Griffith, B., Smaldone, G.C., Iacono, A., 2010. Inhaled cyclosporine and pulmonary function in lung transplant recipients. J. Aerosol Med. Pulm. Drug Deliv. 23, 31–39.
Heng, D., Cutler, D.J., Chan, H.-K., Yun, J., Raper, J.A., 2008. What is a suitable dissolution method for drug nanoparticles? Pharm. Res. 25, 1696–1701.
Iacono, A.T., Corcoran, T.E., Griffith, B.P., Grgurich, W.F., Smith, D.A., Zeevi, A., Smaldone, G.C., McCurry, K.R., Johnson, B.A., Dauber, J.H., 2004. Aerosol cyclosporin therapy in lung transplant recipients with bronchiolitis obliterans. Eur. Respir. J. 23, 384–390.
Iacono, A.T., Johnson, B.A., Grgurich, W.F., Youseff, J.G., Corcoran, T.E., Seiler, D.A., Dauber, J.H., Smaldone, G.C., Zeevi, A., Yousem, S.A., Fung, J.J., Burckart, G.J., McCurry, K.R., Griffith, B.P., 2006. A randomized trial of inhaled cyclosporine in lung-transplant recipients. N. Engl. J. Med. 354, 141–150.
Iacono, A.T., Keenan, R.J., Duncan, S.R., Smaldone, G.C., Dauber, J.H., Paradis, I.L., Ohori, N.P., Grgurich, W.F., Burckart, G.J., Zeevi, A., Delgado, E., O'Riordan, T.G., Zendarsky, M.M., Yousem, S.A., Griffith, B.P., 1996. Aerosolized cyclosporine in lung recipients with refractory chronic rejection. Am. J. Respir. Crit. Care Med. 153, 1451–1455.
Iacono, A.T., Smaldone, G.C., Keenan, R.J., Diot, P., Dauber, J.H., Zeevi, A., Burckart, G.J., Griffith, B.P., 1997. Dose-related reversal of acute lung rejection by aerosolized cyclosporine. Am. J. Respir. Crit. Care. Med. 155, 1690–1698.
Kumon, M., Kwok, P.C.L., Adi, H., Heng, D., Chan, H.-K., 2010. Can low-dose combination products for inhalation be formulated in single crystalline particles? Eur. J. Pharm. Sci. 40, 16–24.
Kwok, P.C.L., Tunsirikongkon, A., Glover, W., Chan, H.-K., 2011. Formation of protein nano-matrix particles with controlled surface architecture for respiratory drug delivery. Pharm. Res. 28, 788–796.
Lechuga-Ballesteros, D., Abdul-Fattah, A., Stevenson, C.L., Bennett, D.B., 2003. Properties and stability of a liquid crystal form of cyclosporine—the first reported naturally occurring peptide that exists as a thermotropic liquid crystal. J. Pharm. Sci. 92, 1821–1831.
Liu, Y., Cheng, C., Liu, Y., Prud'homme, R.K., Fox, R.O., 2008a. Mixing in a multi-inlet vortex mixer (MIVM) for flash nano-precipitation. Chem. Eng. Sci. 63, 2829–2842.
Liu, Y., Tong, Z., Prud'homme, R.K., 2008b. Stabilized polymeric nanoparticles for controlled and efficient release of bifenthrin. Pest Manage. Sci. 64, 808–812.
Martindale: The Complete Drug Reference, 2011. Pharmaceutical Press, London.
Merck Index, 2011. Merck & Co., Whitehouse Station, NJ.
Molimard, M., Till, D., Stenglein, S., Singh, D., Krummen, M., 2007. Inhalation devices for long-acting β_2-agonists: efficiency and ease of use of dry powder formoterol inhalers for use by patients with asthma and COPD. Curr. Med. Res. Opin. 23, 2405–2413.
Myrdal, P.B., Karlage, K.L., Stein, S.W., Brown, B.A., Haynes, A., 2004. Optimized dose delivery of the peptide cyclosporine using hydrofluoroalkane-based metered dose inhalers. J. Pharm. Sci. 93, 1054–1061.
O'Riordan, T.G., Iacono, A.T., Keenan, R.J., Duncan, S.R., Burckart, G.J., Griffith, B.P., Smaldone, G.C., 1995. Delivery and distribution of aerosolized cyclosporine in lung allograft recipients. Am. J. Respir. Crit. Care Med. 151, 516–521.
Pharmaxis, 2009. Statutory Annual Report. Pharmaxis Ltd., Frenchs Forest, NSW, Australia.
Pharmaxis, 2010. Media Release: US Food and Drug Administration Approves Aridol. Pharmaxis Ltd., Frenchs Forest, NSW, Australia.
Pitcairn, G.R., Hooper, G., Luria, X., Rivero, X., Newman, S.P., 1997. A scintigraphic study to evaluate the deposition patterns of a novel anti-asthma drug inhaled from the cyclohaler dry powder inhaler. Adv. Drug Deliv. Rev. 26, 59–67.
Rowe, R.C., Sheskey, P.J., Quinn, M.E., 2011. Handbook of Pharmaceutical Excipients. Pharmaceutical Press, London.
Russ, B., Liu, Y., Prud'homme, R.K., 2010. Optimized descriptive model for micromixing in a vortex mixer. Chem. Eng. Commun. 197, 1068–1075.
Srichana, T., Martin, G.P., Marriott, C., 1998. Dry powder inhalers: the influence of device resistance and powder formulation on drug and lactose deposition in vitro. Eur. J. Pharm. Sci. 7, 73–80.
Zijlstra, G.S., Rijkeboer, M., van Drooge, D.J., Sutter, M., Jiskoot, W., van de Weert, M., Hinrichs, W.L.J., Frijlink, H.W., 2007. Characterization of a cyclosporine solid dispersion for inhalation. AAPS J. 9, E190–E199.